

Apoptosis induced by low-level laser in polymorphonuclear cells of acute joint inflammation: comparative analysis of two energy densities

Lúcia Mara Januário dos Anjos¹ · Adenilson de Souza da Fonseca² · Jacy Gameiro³ · Flávia de Paoli¹

Received: 20 September 2016 / Accepted: 14 March 2017 / Published online: 5 April 2017
© Springer-Verlag London 2017

Abstract Anti-inflammatory property of low-level laser therapy (LLLT) has been widely described in literature, although action mechanisms are not always clarified. Thus, this study aimed to evaluate apoptosis mechanisms in the LLLT anti-inflammatory effects on the arthritis experimental model in vivo at two different energy densities (3 and 30 Jcm⁻²). Arthritis was induced in mice by zymosan solution, animals were distributed into five groups, and morphological analysis, immunocytochemistry and gene expressions for apoptotic proteins were performed. Data showed an anti-inflammatory effect, DNA fragmentation in polymorphonuclear (PMN) cells and alteration in gene expression of proteins related to apoptosis pathways after LLLT. p53 gene expression increased at both energy densities, Bcl2 gene expression increased at 3 Jcm⁻², and Bcl2 tissue expression decreased at 30 Jcm⁻². In addition, apoptosis was restricted to PMN cells.

Results suggest that apoptosis in PMN cells comprise part of LLLT anti-inflammatory mechanisms by disbalance promotion between expression of pro-apoptotic (Bax and p53) and anti-apoptotic (Bcl-2) proteins, with pro-apoptotic gene expression selectively in PMN cells.

Keywords LLLT · Apoptosis · p53 · Bcl2 · Polymorphonuclear cells

Introduction

Arthritis is an inflammatory pathology affecting the joints, considered an important cause of physical disability worldwide. Characterized by synovial inflammation (synovitis) and joint architecture changes, inflammatory and degenerative arthritis is furthermore involved in several chronic conditions such as osteoarthritis and rheumatoid arthritis. Synovitis begins with leukocyte influx into the synovial compartment, resulting in cell hyperplasia at specific site. Inflammatory cell infiltration into synovial exudates, mainly polymorphonuclear (PMN), is one of the main factors leading to articular damages being a hallmark of arthritis [1–3].

PMN cells commonly present a very short half-life and die quickly; however, in an inflammatory process, death through apoptosis is prevented by inflammatory signals, which are able to intensify the chronic arthritis degenerative processes, as observed in RA [4, 5].

Apoptosis is considered a vital component of various processes including normal cell turnover, proper development and functioning of the immune system. Apoptosis mechanisms are highly complex, involving dependent energy molecular signaling which could be initiated by two distinct pathways: the extrinsic or death receptor pathway (via Fas and Fas ligand-FasL) and the intrinsic or mitochondrial pathway (via

Electronic supplementary material The online version of this article (doi:10.1007/s10103-017-2196-8) contains supplementary material, which is available to authorized users.

✉ Lúcia Mara Januário dos Anjos
luciamara.anjos@ufjf.edu.br

- ¹ Departamento de Morfologia, Instituto de Ciências Biológicas, Universidade Federal de Juiz de Fora, Rua José Lourenço Kelmer, s/n-Campus Universitário, São Pedro, Juiz de Fora, Minas Gerais 36036900, Brazil
- ² Departamento de Biofísica e Biometria, Instituto de Biologia Roberto Alcântara Gomes, Universidade do Estado do Rio de Janeiro, Rua São Francisco Xavier, 524, Maracanã, Rio de Janeiro 20550900, Brazil
- ³ Departamento de Microbiologia, Parasitologia e Imunologia, Instituto de Ciências Biológicas, Universidade Federal de Juiz de Fora, Rua José Lourenço Kelmer, s/n-Campus Universitário, Juiz de Fora, Minas Gerais 36036900, Brazil

pro-apoptotic Bcl-2 protein family, as Bax). Both pathways promote mitochondrial outer membrane permeabilization and release of cytochrome c, thereby triggering apoptosis execution events by caspases. The effector caspases activated promote cytoskeleton reorganization and chromosomal DNA degradation by endonucleases, resulting in cell disintegration and apoptotic body formation [6, 7].

Balance between anti-apoptotic (Bcl-2, Bcl-x, Bcl-XL, Bcl-XS, Bcl-w, and BAG) and pro-apoptotic (Bcl-10, Bax, Bak, Bid, Bad, Bim, Bik, and Blk) Bcl2 family members would determine for cellular sensitivity or resistance to various apoptotic stimuli [8] which is an important issue for many pathological conditions. In addition, the tumor suppressor protein p53 plays a critical role in the regulation of the Bcl-2 protein family since it indirectly regulates transcription of Bax genes, providing connection of this tumor suppressor with the apoptosis pathways [9].

Studies have suggested positive performance of low-level light therapy (LLLT) in rheumatic disorder treatments, such as in arthritis, promoting an anti-inflammatory, tissue repair, and analgesia effects [10]. LLLT is a form of phototherapy involving the application of low intensity radiation in red to near-infrared spectrum to treat several diseases. LLLT biostimulation effects are related to alteration of biochemical reactions leading to cellular function modifications. There is evidence indicating that LLLT could induce photochemical interactions, acting on cells through cytochrome c oxidase, and increasing ATP, reactive oxygen, and nitrogen species, energy availability, and signal transduction [11–13]. Moreover, LLLT could also cause an upregulation of various genes related to transcription factors, immune/inflammation, cytokines, and certain proliferation and cell death genes [14, 15].

Notwithstanding in the therapeutic protocols which have been successfully used, the molecular and cellular mechanisms involved in LLLT ability to solve inflammatory processes have not been completely understood yet. Thus, the aim of this study was investigating apoptosis mechanisms in anti-inflammatory effects of two energy densities of LLLT on an experimental arthritis model.

Material and methods

All experimental procedures were submitted and approved by the Ethical Committee of the Universidade Federal de Juiz de Fora (protocol number 039/2014) and conducted in accordance with international ethical standards. Male C57BL/6 mice, 8–10 weeks old, weighting 24–28 g each, were housed, six per cage with free access to laboratory diet and water. Animals were kept in a 12:12 h light/dark cycle (lights on from 6:00 AM to 6:00 PM) in a temperature-controlled room ($25^{\circ} \pm 2^{\circ}\text{C}$). Animals were randomly distributed into five groups ($n = 6$):

- CTR. Control group (joint submitted to 10 μL of sterile PBS injection).
- ZY. Untreated group (joint submitted to inflammation induction with zymosan and untreated).
- ZY + DEXA. Treated with dexamethasone (joint submitted to inflammation induction with zymosan and treated with dexamethasone).
- ZY + 3 Jcm^{-2} . Treated with LLLT at 3 Jcm^{-2} energy density (joint submitted to inflammation induction with zymosan and treated with LLLT at 3 Jcm^{-2} energy density).
- ZY + 30 Jcm^{-2} . Treated with LLLT at 30 Jcm^{-2} energy density (joint submitted to inflammation induction with zymosan and treated with LLLT at 30 Jcm^{-2} energy density).

Zymosan-induced arthritis

Experimental protocol of arthritis followed a previous report of successful zymosan-induced joint inflammation [16]. Briefly, a solution containing 180 μg zymosan A from *Saccharomyces cerevisiae* (Sigma Chemical Company, USA) dissolved in 10 μL of sterile phosphate buffer solution (PBS) was injected into the region near talocrural and subtalar joints (right and left) of mouse hind limbs. For control, 10 μL of sterile PBS was injected in the same area. All procedures were performed using anesthesia, a mix of 80 mg kg^{-1} ketamine (Syntec, Brazil), and 20 mg kg^{-1} xylazine (Syntec, Brazil) intraperitoneally.

Low-level laser device

A therapeutic low-level infrared laser (aluminum gallium arsenide (AlGaAs)) was used for the experimental procedures. It was purchased from HTM Indústria de Equipamentos Eletroeletrônicos Ltda (Brazil), with 830 nm emission, output power at 10 mW, 0.05 cm^2 laser beam area, power density at 0.2 Wcm^{-2} , energy densities at 3 and 30 Jcm^{-2} (total energy of 150 and 1500 mJ were delivered after 15 and 150 s, respectively), at continuous wave emission mode.

Dexamethasone treatment

In order to compare the anti-inflammatory effects between laser and corticosteroids, commonly used for arthritis treatment, the ZY + DEXA group was treated with dexamethasone (Aché Pharmaceutical Laboratory, Brazil) intraperitoneally (4 mg kg^{-1}). The treatments, LLLT exposure (to ZY + 3 Jcm^{-2} and ZY + 30 Jcm^{-2} groups) and dexamethasone administration (to ZY + DEXA group) were performed 4 times: 5, 29, 53, and 77 h after zymosan administration. 5 h after joint inflammation induction with zymosan, six animals were euthanized in order to confirm the presence of an inflammatory process and their cell types in the joint

region (supplementary material), since the treatments had been started at this time point. 24 h after the last laser irradiation and dexamethasone treatment (101 h/4 days after zymosan administration), the five groups were euthanized, and their ankles were removed and the skin were dissected. Right ankles were used for histological procedure analysis, Immunohistochemical and TUNEL POD analysis and left ankle for mRNA expression analysis.

Histological procedures

The dissected samples were fixed in 4% paraformaldehyde/PBS solution for 24 h, decalcified in 5% nitric acid for 48 h, dehydrated, and embedded in histosec® paraffin (Merck, Germany). Sagittal sections (4 µm thickness) were stained with hematoxylin and eosin (H&E) and were used for immunohistochemical and TUNEL POD analysis.

Immunohistochemical assessment

Immunohistochemical assessment (IHC) detection was carried out on 4-µm-thick deparaffinized sections. Before IHC, sections were subjected to heat-induced epitope retrieval by incubation in a 0.01 M sodium citrate solution (pH 6), at microwave oven, during 20 min and followed by a 20 min cool-down. Endogenous peroxidase activity was blocked using 3% H₂O₂ diluted in absolute methanol, followed by 1.5% blocking serum of rabbit ABC Staining System (Santa Cruz Biotechnology, USA). A primary polyclonal antibody anti-Bcl2 (Santa Cruz Biotechnology, USA) was used, was diluted as suggested by the manufacturer, was and performed overnight at 4 °C. An appropriate secondary biotinylated antibody of rabbit ABC Staining System (Santa Cruz Biotechnology, USA) was used during 30 min, at room temperature, followed by ABC-Peroxidase solution, containing 3–3'-diaminobenzidine (Sigma Aldrich, USA) chromogen during 10 min, at room temperature. The sections were counterstained using methyl green. As a negative control, sections were incubated in the absence of primary antibody.

DNA fragmentation

Apoptotic cells in mouse ankle joint samples were detected using a TUNEL POD assay (Roche, Germany) according to the manufacturer's manual. After deparaffinization and permeabilization, the tissue sections were incubated in proteinase K for 15 min at room temperature. The sections were then incubated with the TUNEL reaction mixture which contains terminal deoxynucleotidyl transferase (TdT) and fluorescein-dUTP at 37 °C for 1 h. After washing three times with PBS, the sections were incubated with Converter-POD containing anti-fluorescein antibody conjugated with horse-radish peroxidase (POD) at room temperature for 30 min. After washing three times with

PBS, these sections were incubated with 3–3'-diaminobenzidine (Sigma Aldrich, USA) for 10 min at room temperature (25 °C), and then counterstained with methyl green.

Image analyses

Morphological analyses and quantitative assessments were performed using an Olympus microscope (BX53F), equipped with U-PlanFL N 4/0.13, 10/0.30, 40/0.75, and 100/0.85 objectives. The images were captured with an Olympus DP73 camera, using cellSens Imaging software (5.1 version, Olympus, EUA). For quantitative analysis, the 100/0.85 objective was used and, under these conditions, 1 pixel corresponded to 440 nm. Image Pro Plus software (Media Cybernetics, Inc.) was used for measurements of inflammatory infiltration area and cellular density (mean of cell number in 5 fields × infiltration area) and positive cell labeling quantification of immunohistochemistry and TUNEL POD.

Total RNA extraction, complementary DNA synthesis, and real-time quantitative polymerase chain reaction assay

Tissue fragments from mouse left hind limb were macerated after immersion in liquid nitrogen, and total RNA was extracted by phenol-buffered technique. Briefly, TRIzol® reagent (Invitrogen, USA) was added and centrifuged (12,000 rpm, 4 °C, 10 min). Supernatants were transferred to other tubes, chloroform was added, mixtures were centrifuged (12,000 rpm, 4 °C, 15 min), aqueous phases were transferred to other tubes, and isopropanol was added. After incubation (room temperature, 15 min), mixtures were centrifuged (12,000 rpm, 4 °C, 10 min), supernatants were discarded, and precipitate was washed with ethanol-DEPC (80% ethanol, DEPC 0.1%) solution and centrifuged. Supernatants were withdrawn and total RNA was reconstituted in water-DEPC (0.1%) solution. RNA concentration and purity were determined on a spectrophotometer by calculating optical density ratio at a 260/280 nm wavelength ratio. Then, 2 µg of total RNA were transcribed to complementary DNA (cDNA) using the High-Capacity cDNA Reverse Transcription Kit (Applied Biosystems, USA) following manufacturer's guidelines.

The primers for real-time quantitative polymerase chain reaction (RT-qPCR) were designed using the Primer 3 program [17], on different exons in order to avoid the possibility of genomic DNA contamination. The primers of genes used here (encoding proteins involved in signaling pathways for apoptosis) are described in supplementary material (Table S1). β-actin was used as internal control (forward: CATCCGTAAAGACCTCTATGCC; reverse: GGAGCCAG AGCAGTAATCTC).

RT-qPCR assay was performed in StepOnePlus™ Real-Time PCR System instrument (Applied Biosystems, USA)

under the following conditions: 40 cycles; in each cycle, initial denaturation at 95 °C for 10 min, denaturation at 95 °C for 15 s, and annealing of the primers and extension at 60 °C for 1 min.

For gene expression analysis by RT-qPCR the Delta-Delta Ct method ($\Delta\Delta Ct$) was used [18]. Internal normalization was performed by β -actin and untreated samples (ZY) were used to calculate the $\Delta\Delta Ct$.

Statistical analysis

Statistical analyses were performed using InStat3.0 and GraphPad Prism 5.0 (GraphPad Software Inc., USA). Data are expressed as mean \pm SD. The immunohistochemical, TUNEL POD and the morphological analyses were further evaluated through one-way ANOVA tests followed by Bonferroni tests. For other data, the differences in mean values

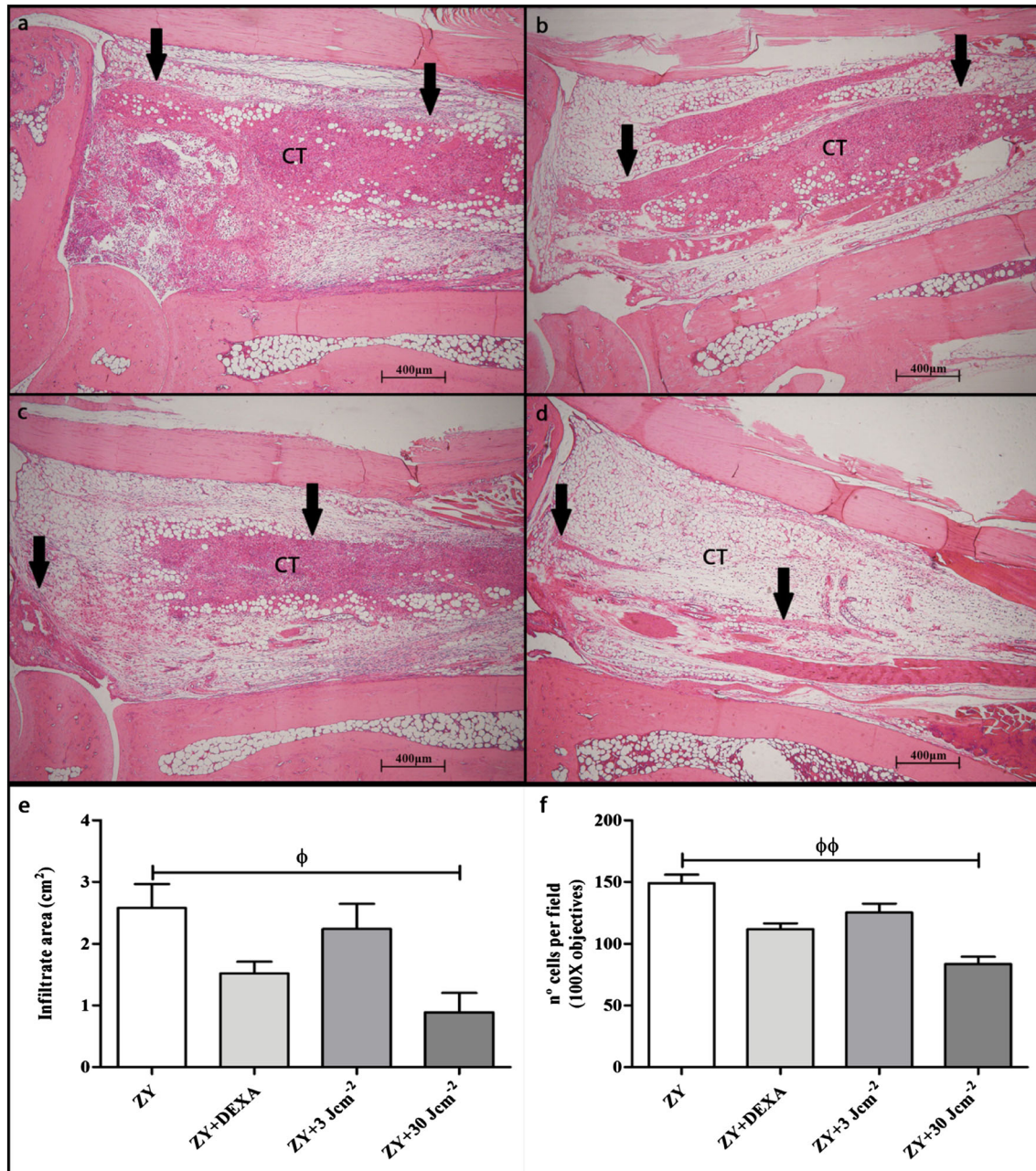


Fig. 1 Representative photomicrographs of mouse ankle and subtalar joints and adjacent connective tissues (CT) 101 h/4 days after zymosan inflammation induction (H&E staining $\times 4$) and infiltrate quantifications. **a** Photomicrograph of untreated group (ZY). **b** Photomicrograph of dexamethasone-treated (ZY + DEXA). **c** Photomicrograph of LLLT

3 Jcm⁻² (ZY + 3 Jcm⁻²). **d** Photomicrograph of LLLT 30 Jcm⁻² (ZY + 30 Jcm⁻²). **e** Infiltrate area. **f** Cell density of inflammatory process in connective tissue. *Arrows* indicate inflammatory infiltrates. (ϕ) $p < 0.05$ and ($\phi\phi$) $p < 0.01$ when compared with untreated group (ZY)

between groups were analyzed by two-tailed Student's *t* test. Differences were considered significant when $p < 0.05$.

Results

Morphological analysis

Zymosan administration induced an inflammatory process in mouse subtalar and talocrural joints characterized by influx of inflammatory cells in synovial tissues and their adjacent connective tissue. 5 h after the zymosan-induction, cell infiltrate was characterized by presence of PMN cells, particularly neutrophils. After 4 days and 4 treatment sessions, neutrophils, macrophages, lymphocytes, and intense deposition of fibrous tissue could be observed (Figure S2). Controls have not shown any inflammatory process. No morphological alterations in adjacent tissues of inflammatory process were observed in all groups.

For ZY + DEXA, ZY + 3 Jcm⁻² and ZY + 30 Jcm⁻² groups was observed a decrease in inflammatory infiltrate. However, only in group ZY + 30 Jcm⁻², statistically significant differences were observed in infiltrate area ($p < 0.05$) and cell density, when compared to untreated group (ZY) (Fig. 1).

Laser effect on DNA fragmentation rate of inflammatory cells

Positive labeling for DNA fragmentation, analyzed by TUNEL POD assay, was observed predominantly in

inflammatory cells present in zymosan-induced groups. Positive labeling was mainly observed in group ZY + 30 Jcm⁻² ($p < 0.001$), followed by group ZY + 3 Jcm⁻² ($p < 0.01$) when compared to untreated group (ZY) (Fig. 2).

LLLT effects on gene expression of proteins involved in apoptosis pathways

In order to analyze which mechanisms were related to cell death observed selectively in PMN cells after laser exposure, mRNA expression from genes involved in apoptosis pathways, as well as those involved in their regulations were performed by RT q-PCR.

When compared with untreated group (ZY), group ZY + 3 Jcm⁻² presented a significant increase in mRNA expression from FasL, CASP-9, CASP-6, Bax, p53, Bid, and Bcl2 genes ($p < 0.001$) (Fig. 3a), while group ZY + 30 Jcm⁻² showed a significant increase of mRNA expression from FasL ($p < 0.001$), Bax ($p < 0.001$), Fas ($p < 0.01$), CASP-3 ($p < 0.01$), CASP-6 ($p < 0.01$), p53 ($p < 0.01$), Bid ($p < 0.01$), Bad ($p < 0.01$), and Apaf-1 ($p < 0.01$) (Fig. 3b). Group ZY + DEXA did not present a significant alteration ($p > 0.05$) in mRNA expression from all apoptosis genes evaluated (Figure S3).

LLLT effects on Bcl2 protein and mRNA expression

In the immunohistochemical assessment, Bcl2 protein expression was predominant in PMN cells (Fig. 4). Quantitative analysis showed that group ZY + 30 Jcm⁻² presented fewer

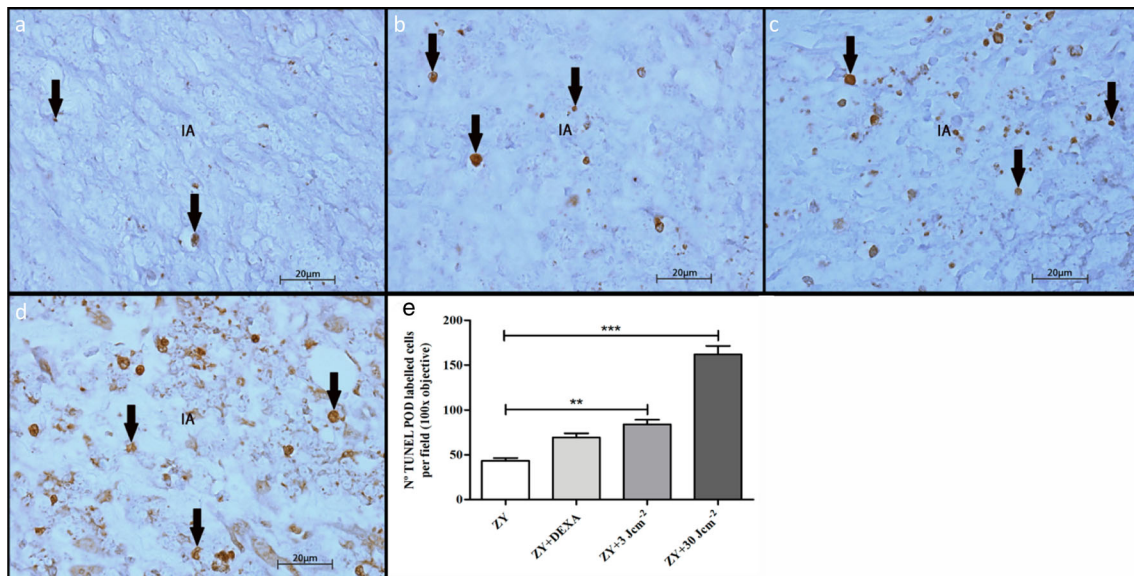


Fig. 2 Photomicrographs ($\times 100$) of joint infiltrate area (IA), demonstrating positive TUNEL POD labeling in cells displaying DNA fragmentation (arrows) and TUNEL POD positive labeling quantification. **a** Photomicrograph of untreated group (ZY). **b** Photomicrograph of group treated with dexamethasone (ZY + DEXA).

c Photomicrograph of group treated with LLLT at 3 Jcm⁻² (ZY + 3 Jcm⁻²). **d** Photomicrograph of group treated with LLLT at 30 Jcm⁻² (ZY + 30 Jcm⁻²). **e** TUNEL POD positive labeling quantification in infiltrate area. (**) $p < 0.01$ and (***) $p < 0.001$ when compared to untreated group (ZY)

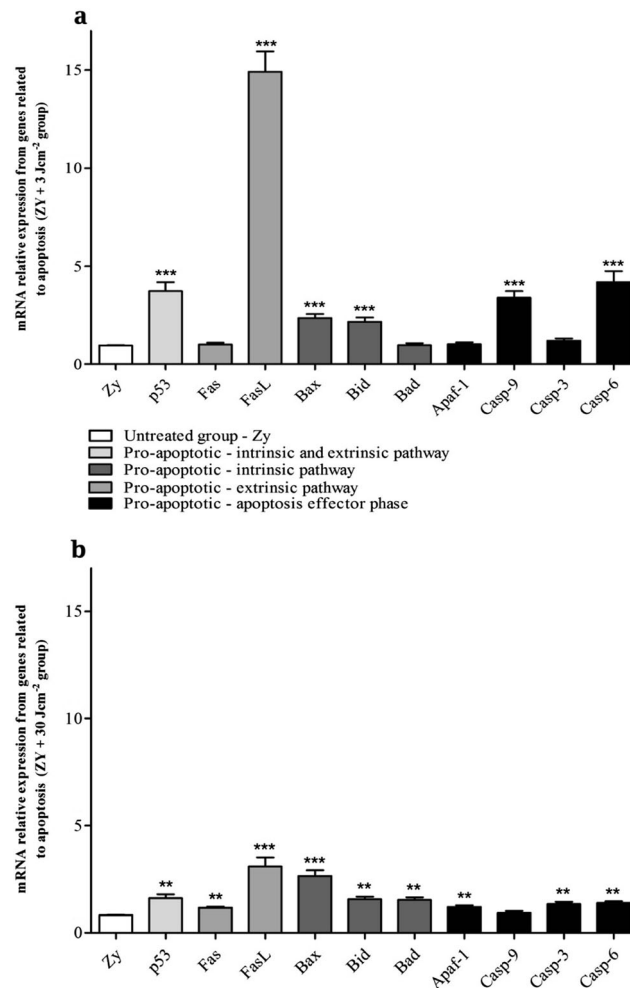


Fig. 3 **a** mRNA relative expression of genes related to apoptosis in mouse ankle joints after LLLT at 3 Jcm⁻² (ZY + 3 Jcm⁻²). **b** mRNA relative expression from genes related to apoptosis in mouse ankle

joints after LLLT at 30 Jcm⁻² (ZY + 30 Jcm⁻²). β -actin was used as an internal control. (***) $p < 0.001$ and (**) $p < 0.01$ when compared to untreated group (ZY)

cells that are positive labeled than the untreated group (ZY) ($p < 0.01$), while in group ZY + 3 Jcm⁻² showed an increase, but not statistically significant ($p > 0.05$) of Bcl2 protein expression in tissue. The Bcl2 mRNA up-expression ($p < 0.001$) was showed in the ZY + 3 Jcm⁻² group, while in group ZY + 30 Jcm⁻² Bcl2 mRNA expression was similar to results showed by untreated group (ZY) (Fig. 5).

Since group ZY + DEXA did not present an increase in DNA fragmentation of inflammatory cells (Fig. 5), as well as alterations in mRNA expression of Bcl2 if compared to untreated group (ZY) (Figure S3), IHC and RT q-PCR to Bcl2 were not performed for this group.

Discussion

Anti-inflammatory effect of LLLT has been widely described in the literature [10, 19, 20] and has been associated to alteration of prostaglandin levels, vascular permeability, and transcription

factor NF- κ B modulation. [21–23] Further, research works have shown that the anti-inflammatory effect of LLLT could also be involved in apoptosis induction in PMN cells [13, 24, 25].

In the present study, it could be observed that the inflammatory process treatment using low-level laser at 30 Jcm⁻² (ZY + 30 Jcm⁻²) decreases the inflammatory area, as well as the number of infiltrate cells. Additionally, DNA fragmentation is strongly present in inflammatory cells after laser irradiation for both laser energy densities evaluated. As these cells show DNA fragmentation, cell death could occur by the apoptosis process, often involving an intracellular signaling cascade and action of effectors caspases, such as caspase 3 and caspase 6 [26]. These results indicate that the LLLT anti-inflammatory mechanisms observed in this study are associated with apoptosis induction in PMN cells, mainly those observed at the highest energy density (ZY + 30 Jcm⁻²).

Comparing with the untreated group (ZY), the group treated with the lower energy density (ZY + 3 Jcm⁻²) did not present a significant inflammatory process reduction ($p > 0.05$), even

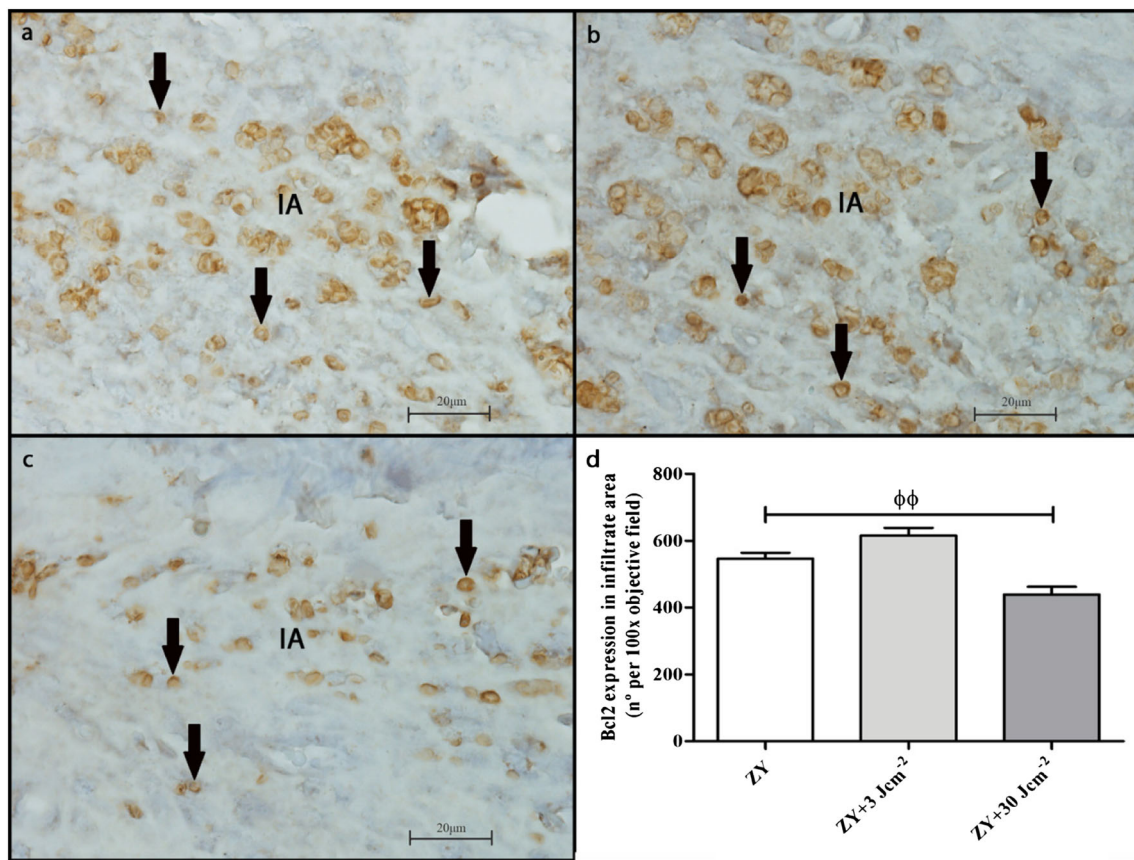


Fig. 4 Photomicrographs ($\times 100$) of joint infiltrate area (IA), demonstrating positive Bcl2 IHC labeled cells (arrows) and Bcl2 positive labeling quantification. **a** Photomicrograph of untreated group (ZY). **b** Photomicrograph of group treated with LLLT at 3 Jcm^{-2} (ZY +

3 Jcm^{-2}). **c** Photomicrograph of group treated with LLLT at 30 Jcm^{-2} (ZY + 30 Jcm^{-2}). **d** Bcl2 positive labeling quantification in infiltrate area. ($\phi\phi$) $p < 0.01$ when compared to untreated group (ZY)

though high rates of DNA fragmentation had been observed in PMN cells ($p < 0.01$). Taken together, these results could indicate that induction of inflammatory cell death in group ZY + 3 Jcm^{-2} , could be in progress, but slower than that observed in group ZY + 30 Jcm^{-2} .

In all the procedures, the group treated with dexamethasone (ZY + DEXA) showed no significant differences ($p > 0.05$) in their results if compared with untreated group (ZY), demonstrating low efficacy in resolution of the inflammatory process induced by zymosan when compared to LLLT treated groups.

The photobiological effects of LLLT occur following absorption of light photons by chromophores related to mitochondrial respiratory chain (cytochrome c oxidase, for example), which produces a photosignal, subsequently transduced into the cell. This photosignaling involves transient free radical production, increases adenosine triphosphate (ATP), and modulates cellular redox potential, which could induce redox-sensitive transcription factors, e.g., nuclear factor kappa B (NF- κ B) and p53. LLLT could also generate singlet oxygen stimulating processes, such as RNA and DNA synthesis. Therewith, photobiological effects of LLLT are observed, as increase of cell migration, cytokine levels, growth factors,

inflammatory mediator modulation, and increase of tissue oxygenation [14, 27–30].

On the other hand, the p53 activation induces cell growth arrest or apoptosis, and it is one of the key tumor suppressors, modulating both intrinsic and extrinsic apoptosis pathways in response to various stressors, including DNA damage, hypoxia, and oncogenetic activation. In the extrinsic pathway, overexpressed p53 not only stimulates Fas transcription, but also promotes the trafficking of Fas receptor from Golgi to cytoplasmic membrane, allowing rapidly sensitized cells to Fas and inducing apoptosis. In addition, in the intrinsic pathway, p53 acts stimulating pro-apoptotic Bax, Bid and Bad gene transcription, and direct activating caspase-8. Also, p53 stimulates Apaf-1 and CASP-6 gene expression, whose proteins are related to apoptosis signaling effector phase [31–33].

p53 activation could occur by changes in intracellular redox potential, as a consequence of LLLT, resulting in increase of pro-apoptotic Bax, Bid, Bad, Fas, Apaf-1, and CASP-6 gene expression observed in this study. In fact, p53 upregulates gene expression coding of these proteins. [31–33] These findings support the hypothesis that LLLT activates and upregulates p53 gene expression in PMN cells,

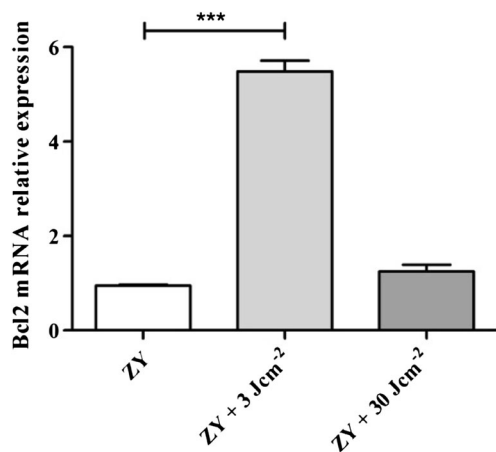


Fig. 5 mRNA relative expression of Bcl2 gene in joint infiltrate area. ZY untreated group, ZY + 3 Jcm⁻² group treated with LLLT at 3 Jcm⁻², ZY + 30 Jcm⁻² group treated with LLLT at 30 Jcm⁻². (***) $p < 0.001$, when compared with untreated group (ZY)

promoting an imbalance between the expression of anti- and pro-apoptotic proteins associated with death signaling. Changes in cell redox potential caused by LLLT could be related not only to apoptosis activation, but also to DNA damage, leading to p53 activation. It has already been described that ROS production increased in response to LLLT could induce DNA repair mechanisms, suggesting that LLLT induces sublethal lesions in DNA [34, 35].

In addition, LLLT photosignaling products could generate others down-stream effects related to apoptosis pathways, as CASP-3 and FasL gene up-expression, which was observed in our study (Fig. 3a, b). FasL up-expression occurs after forkhead box transcription factor (class O-FoxO) activation, which could be also induced by increase of ROS levels [36, 37].

However, the decision about PMN cell survival was probably assigned to Bcl2 expression. At higher energy density (30 Jcm⁻²), PMN cells concomitantly showed a decrease of Bcl2 tissue expression and up-expression of pro-apoptotic proteins. On the other hand, lower energy density (3 Jcm⁻²) increases Bcl2 gene expression and shows a tendency to increase Bcl2 tissue expression, which could preserve PMN cells alive. It is possible that different responses after laser energy densities are only temporal, in the highest energy densities (as 30 Jcm⁻²) the resolution of inflammatory process by apoptosis induction in PMN cells is faster than with the lowest energy densities (3 Jcm⁻²).

It is already expected that transcription factors and cell-signaling pathways, which promote apoptosis, could be activated after higher light exposure and even LLLT at high energy densities by increasing of free radical production [38]. The type of cell analyzed (PMN cells) must also be taken into consideration, which is probably responsible for these findings. The additional mechanism for the free radical production presented by these

cells can be a plausible explanation for the greater, selective effects of LLLT on PMN cells.

Conclusion

The higher energy density (30 Jcm⁻²) is capable of reducing the inflammatory process by PMN apoptosis induction, while the lower energy density (3 Jcm⁻²) could also induce apoptosis in PMN; however, this process seems to be slower. The results suggest that apoptosis in PMN cells comprises part of LLLT anti-inflammatory mechanisms and could be a consequence of the balance alteration between expression of pro-apoptotic (Bax and p53) and anti-apoptotic (Bcl-2) proteins in these cells.

Acknowledgements This study was supported by Conselho Nacional de Pesquisa e Desenvolvimento-CNPq (process number APQ 474405/2013-3) and Fundação de Amparo à Pesquisa do Estado de Minas Gerais-FAPEMIG (process number APQ 00432-13).

Compliance with ethical standards

Conflict of interest The authors wish to declare no conflict of interests.

References

- Pap T, Korb-Pap A (2015) Cartilage damage in osteoarthritis and rheumatoid arthritis—two unequal siblings. *Nat Rev Rheumatol* 11(10):606–615
- Firestein GS (2003) Evolving concepts of rheumatoid arthritis. *Nature* 423(6937):356–361
- McInnes IB, Schett G (2007) Cytokines in the pathogenesis of rheumatoid arthritis. *Nat Rev Immunol* 7(6):429–442
- Pope RM (2002) Apoptosis as a therapeutic tool in rheumatoid arthritis. *Nat Rev Immunol* 2(7):527–535
- Chitnis D, Dickerson C, Munster AM, Winchurch RA (1996) Inhibition of apoptosis in polymorphonuclear neutrophils from burn patients. *J Leukoc Biol* 59(6):835–839
- Elmore S (2007) Apoptosis: a review of programmed cell death. *Toxicol Pathol* 35(4):495–516
- Martinou JC, Youle RJ (2011) Mitochondria in apoptosis: Bcl-2 family members and mitochondrial dynamics. *Dev Cell* 21(1):92–101
- Reed JC (2000) Mechanisms of apoptosis. *Am J Pathol* 157(5):1415–1430
- Schuler M, Green DR (2001) Mechanisms of p53-dependent apoptosis. *Biochem Soc Trans* 29(Pt 6):684–688
- Brosseau L, Robinson V, Wells G, Debie R, Gam A, Harman K, Morin M, Shea B, Tugwell P (2005) Low level laser therapy (classes I, II and III) for treating rheumatoid arthritis. *Cochrane Database Syst Rev* 19(4):CD002049
- Gao X, Xing D (2009) Molecular mechanisms of cell proliferation induced by low power laser irradiation. *J Biomed Sci* 16(1):4
- Tafur J, Mills PJ (2008) Low-intensity light therapy: exploring the role of redox mechanisms. *Photomed Laser Surg* 26(4):323–328
- Karu TI (2010) Multiple roles of cytochrome *c* oxidase in mammalian cells under action of red and IR-A radiation. *IUBMB Life* 62(8):607–610

14. Karu TI (2008) Mitochondrial signaling in mammalian cells activated by red and near-IR radiation. *Photochem Photobiol* 84(5):1091–1099
15. Zhang Y, Song S, Fong CC, Tsang CH, Yang Z, Yang M (2003) cDNA microarray analysis of gene expression proteins in human fibroblast cells irradiation with red light. *J Invest Dermatol* 120(5):849–857
16. Dimitrova P, Ivanovskaa N, Schwaebleb W, Gyurkovskaa V, Stover C (2010) The role of properdin in murine zymosan-induced arthritis. *Mol Immunol* 47(7–8):1458–1466
17. Untergasser A, Cutcutache I, Koressaar T, Ye J, Faircloth BC, Remm M, Rozen SG (2012) Primer3—new capabilities and interfaces. *Nucleic Acids Res* 40(15):e115
18. Livak KJ, Schmittgen TD (2001) Analysis of relative gene expression data using real-time quantitative PCR and the 2^{(-Delta Delta C(T))} method. *Methods* 25(4):402–408
19. Kingsley JD, Demchak T, Mathis R (2014) Low-level laser therapy as a treatment for chronic pain. *Front Physiol* 5:306
20. Bjordal JM, Johnson MI, Lopes-Martins RAB, Bogen B, Chow R, Ljunggren AE (2007) Short-term efficacy of physical interventions in osteoarthritic knee pain. A systematic review and meta-analysis of randomised placebo-controlled trials. *BMC Musculoskelet Disord* 8:51
21. de Jesus JF, Spadacci-Morena DD, dos Anjos Rabelo ND, Pinfieldi CE, Fukuda TY, Plapler H (2015) Low-level laser therapy in IL-1 β , COX-2, and PGE2 modulation in partially injured Achilles tendon. *Lasers Med Sci* 30(1):153–158
22. Mester A (2013) Laser biostimulation. *Photomed Laser Surg* 31(6):237–239
23. Rizzi CF, Mauriz JL, Freitas Corrêa DS, Moreira AJ, Zettler CG, Filippin LI, Marroni NP, González-Gallego J (2006) Effects of low-level laser therapy (LLLT) on the nuclear factor (NF)- κ B signaling pathway in traumatized muscle. *Lasers Surg Med* 38(7):704–713
24. Morgan MC, Rashid RM (2009) The effect of phototherapy on neutrophils. *Int Immunopharmacol* 9(4):383–388
25. Hemvani N, Chitnis DS, Bhagwanani NS (1999) Nitrogen and he-ne laser exposure increases apoptotic death rate for monocytes from human blood. *Laser Ther* 11(1):19–25
26. Nagata S (2000) Apoptotic DNA fragmentation. *Exp Cell Res* 256(1):12–18
27. Karu TI (1999) Primary and secondary mechanisms of action of visible to near-IR radiation on cells. *J Photochem Photobiol B* 49(1):1–17
28. Chen ACH, Arany PR, Huang YY, Tomkinson EM, Saleem T, Yull FE, Blackwell TS, Hamblin MR (2011) Low-level laser therapy activates NF- κ B via generation of reactive oxygen species in mouse embryonic fibroblasts. *PLoS One* 6(7):e22453
29. Hamblin MR, Demidova TN (2006) Mechanisms of low level light therapy. *Proc. SPIE* 6140, Mechanisms for Low-Light Therapy, 6140: 614001–12
30. KARU TI (2003) Biomedical photonics handbook. CRC Press, Boca Raton
31. Haupt S, Berger M, Goldberg Z, Haupt Y (2003) Apoptosis—the p53 network. *J Cell Sci* 116(Pt 20):4077–4085
32. Maclachlan TK, El-Deiry WS (2002) Apoptotic threshold is lowered by p53 transactivation of caspase-6. *Proc Natl Acad Sci USA* 99(14):9492–7
33. Rozenfeld-Granot G, Krishnamurthy J, Kannan K, Toren A, Amariglio N, Givol D, Rechavi G (2002) A positive feedback mechanism in the transcriptional activation of Apaf-1 by p53 and the coactivator Zac-1. *Oncogene* 21(10):1469–1476
34. Fonseca AS, Campos VM, Magalhães LA, Paoli F (2015) Nucleotide excision repair pathway assessment in DNA exposed to low-intensity red and infrared lasers. *Braz J Med Biol Res* 48(10):929–938
35. Sergio LPS, Marciano RS, Polignano GAC, Guimarães OR, Geller M, Paoli F, Fonseca AS (2012) Evaluation of DNA damage induced by therapeutic low-level red laser. *J Clin Exp Dermatol Res* 3:166
36. Greer EL, Brunet A (2005) FOXO transcription factors at the interface between longevity and tumor suppression. *Oncogene* 24(50):7410–7425
37. Klotz LO, Sánchez-Ramos C, Prieto-Arroyo I, Urbánek P, Steinbrenner H, Monsalve M (2015) Redox regulation of FoxO transcription factors. *Redox Biol* 6:51–72
38. Huang YY, Chen ACH, Carroll JD, Hamblin MR (2009) Biphasic dose response in low level light therapy. *Dose-Response* 7(4):358–383

Lasers in Medical Science is a copyright of Springer, 2017. All Rights Reserved.